Electrochemical and Solid-State Letters, **11** (9) D69-D71 (2008)
1099-0062/2008/11(9)/D69/3/$23.00 © The Electrochemical Society

Fabrication of ZnO Nanowire Devices via Selective Electrodeposition

Min Zhang,[a,z] Zhaoying Zhou,[a] Xing Yang,[a] Xiongying Ye,[a] and Zhong Lin Wang[b]

[a]*State Key Laboratory of Precision Measurement Technology and Instruments, Department of Precision Instruments and Mechanology, Tsinghua University, Beijing 100084, China*
[b]*School of Materials Science and Engineering, Georgia Institute of Technology, Atlanta, Georgia 30332-0245, USA*

We introduce a solution-based electrodeposition technique that selectively deposits copper only at the contacts between nanowires/nanobelts/nanotubes and the electrodes, while leaving the device surfaces clean. This was achieved using a copper nitrate bath with low covering power. Our method demonstrates an effective, parallel process for achieving stable electric and mechanical contacts for one-dimensional nanomaterial-based devices on a large scale.
 [DOI: 10.1149/1.2943658]

Manuscript submitted March 31, 2008; revised manuscript received May 19, 2008. Published June 18, 2008.

Semiconducting nanowires (NWs) and nanobelts (NBs) are the fundamental building blocks for fabricating unique nanoscale devices, such as field-effect transistors, photoelectronic devices, and chemical sensors.[1-5] The electrical measurement of a field-effect transistor, for example, is largely affected by the type (Schottky or ohmic) of contact and the contact resistance. Achieving a good ohmic contact is essential for exploring the electrical and optoelectronic properties of NWs and NBs. A general approach is a direct deposition of a single NW/NB from solution onto prefabricated electrodes, which usually leads to a high contact resistance and even nonsymmetric contacts at the two ends.[2] A better electrical contact can be achieved by depositing metal on the top of the NW/NB using focused ion beam (FIB) microscopy.[6] FIB-based metal deposition is not only a slow process depositing from one contact to the next but also prohibitive in cost. There are also other approaches to make contact with NWs, such as electron beam lithography,[7,8] focused electron beam,[9] and shadow masking.[10,11] The challenge is still limited to a small number of contacts. Therefore, it is highly desirable to have a parallel process for economically fabricating the NW devices over a large array of contacts.

In this article, we present an approach to make effective contacts between zinc oxide (ZnO) NWs with microelectrodes using a selective copper electrodeposition technique. By carefully selecting the electroplating bath, the copper is deposited only on the electrodes, leaving the ZnO NWs clean. Copper electrodeposition is a main interconnecting technology for ultralarge-scale integration fabrication, as well as for printed-circuit boards. Thus, this local copper deposition technique allows an effective, parallel process for fabricating ZnO NW/NB devives on a large scale. This is of great importance for building functional device systems using NWs/NBs.

The ZnO NWs used in this work were synthesized by a solid–vapor process under controlled conditions without the presence of a catalyst, and were structurally perfect and geometrically uniform.[12] The Au electrode patterns were defined with photolithography on a Si substrate covered with 50 nm thermally oxidized SiO_2. The microelectrodes consisted of two 2 μm wide fingers at a distance of 2 μm. These two fingers were connected to two 500 × 500 μm contacting pads for probe contacts, as shown in Fig. 1. A single NW was "placed" across the electrodes using the micromanipulation technique described in Ref. 11 (Fig. 1a). Because of the relatively weak adhesion force between the NW and the electrodes, the NW was very easy to move or float away into the electrolyte when it immerged into the electrolyte at the beginning of the electrodeposition process. However, this problem can be solved by using an electroadsorption process before electrodeposition. After applying a pulse voltage (V_p = 5 V, f = 1000 Hz) across the two electrodes for a few minutes (Fig. 1b), the ZnO NWs could be absorbed on the electrodes so firmly that no desorption or moving of the NW occurred during electrodeposition. A tiny movement of the NW on the electrodes could be observed at the beginning of applying the voltage, indicating that the NW was adhered on the electrodes by electrostatic force and tighter contacts were formed. Moreover, when applying 5 V voltage, the current passing through the device was 1–5 μA, corresponding to a power of 5–25 μW. For the small contact area (about 10^{-12} m^2) and the volume of the NW (about 10^{-18} m^3), the rise in temperature at the contacts can be large. Therefore, the improvement of the adhesion force between the NW and the electrodes is probably also caused by the thermal annealing occurring at the contact region.

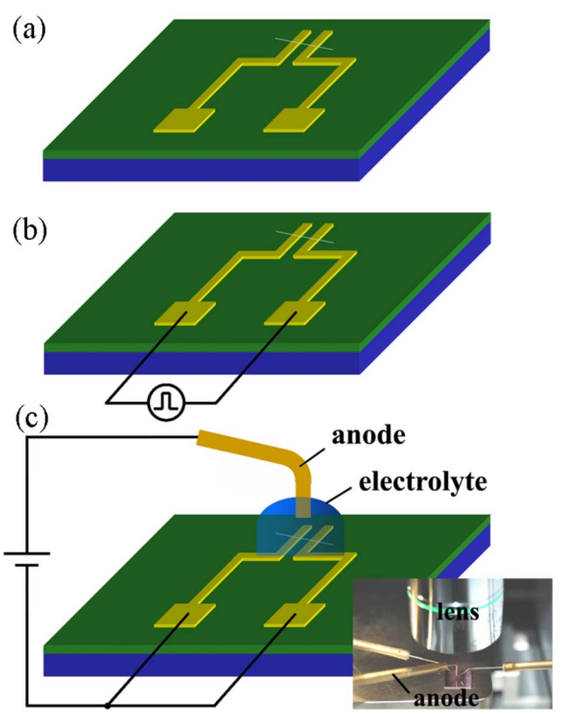

Figure 1. (Color online) Schematic diagrams of the fabrication process of ZnO NW device (not to scale): (a) crossing a single ZnO NW on the patterned electrodes by micromanipulating, (b) applying pulse voltage between the electrodes to achieve electroadsorption of ZnO NW on the electrodes, and (c) the experimental setup of electrodeposition. The patterned electrodes were connected together as the cathode; a pure copper wire was placed above the cathode to serve as the anode. A droplet of plating solution was applied between the cathode and anode to realize electrodeposition. The inset is a photograph of the experimental setup.

[z] E-mail: zminer1229@eyou.com

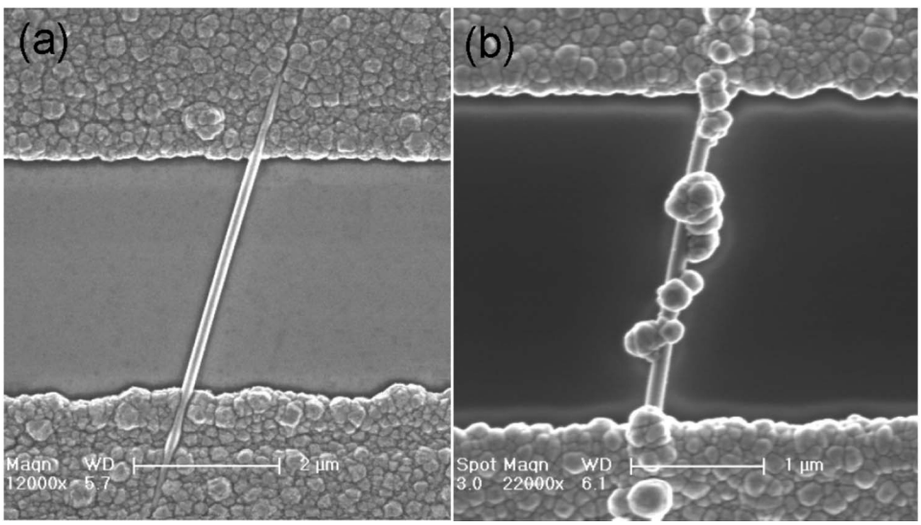

Figure 2. SEM images of copper embedded ZnO NW after electrodeposition using (a) copper nitrate bath and (b) pyrophosphate bath. The electrodeposition conditions of copper nitrate bath are $Cu(NO_3)_2$ 400 g/L, Cl^- 50 ppm, PEG6000 10 ppm, current density 1 A/dm^2, corresponding to a Cu deposition rate of 3–4 nm/s. The electrodeposition conditions of pyrophosphate bath are $Cu_2P_2O_7$ 60 g/L, $K_4P_2O_7 \cdot 3H_2O$ 280 g/L, $NH_3 \cdot H_2O$ 2 mL/L, current density 0.5 A/dm^2, corresponding to a Cu deposition rate of 1–2 nm/s.

The electrodeposition process, as shown in Fig. 1c, was conducted on a probe station with the two finger electrodes connected together as the cathodes and a 0.2 mm diameter pure copper wire with a polished end as the anode. The anode was placed 1 mm above the cathode. After connecting the electrodes to a dc source, a droplet of the plating solution was applied between the cathode and the anode. After deposition, the wafer was rinsed with deionized water, followed by drying at 60°C for 1 h.

Two kinds of electroplating baths were used for copper deposition: pyrophosphate bath and copper nitrate bath. The copper distributions on the ZnO NW/electrode system using different plating baths were investigated by scanning electron microscope (SEM) (Fig. 2). It was found that copper tends to deposit on the NW surface in pyrophosphate solution, forming a cluster of copper particles on the NW (Fig. 2b) and, consequently, deteriorating the performance of the nanodevice. However, when using copper nitrate solution, copper only deposited on the Au electrodes surface (Fig. 2a); therefore, the ZnO NW was enclosed in the electrodes only at the contact region. Transmission electron microscopy (TEM) was used to further examine the ZnO NWs after electrodeposition using copper nitrate solution (Fig. 3). The NW was transferred from the wafer after electrodeposition to a molybdenum grid for TEM observation. No copper particles were observed on the ZnO NW surface under TEM observation (Fig. 3a). Several energy-dispersive X-ray spectroscopy (EDS) spectra were taken from different positions along the ZnO NW, and no copper signature was found in the spectra (Fig. 3c). The carbon signature in the EDS spectrum is from the molybdenum TEM grid coated with a carbon film. The appearance of iron and chromium signatures is perhaps caused by the impurities of the molybdenum grid. To further inspect whether a very thin film of copper was formed on the NW surface or not, a high-resolution TEM image as well as a corresponding electron diffraction pattern was recorded from the edge of the NW (Fig. 3b), showing a single-crystal volume with a clean surface; also, no copper pattern was found in the electron diffraction pattern.

Generally, a metal electrodeposition process is composed of two successive steps: the reduction of metal cations to metal atoms at the cathode surface and the metal crystallization process. In the first step, the reducing reaction will only occur as the cathode overpotential exceeds the reducing potential of the metal ions. In a given electrochemical system, the overpotential is mainly determined by the current density.[13] Due to the geometric and material inhomogeneity of the cathode surface, the distribution of the electrical field, i.e., the distribution of the current on the cathode surface is inhomogeneous, and even quite different in some positions. Plating baths with high covering power have the ability to deposit metal at regions of low current density; therefore, relatively uniform metal coatings can be obtained all over the cathode surface. In low-covering-power baths, the nonuniform cathode current distribution caused by the inhomogeneity of the cathode surface cannot be eliminated, resulting in normally undesired nonuniform or even disconnected coatings. This phenomenon, however, can be utilized in our current work to achieve selective electrodeposition on the electrodes instead of the ZnO NW.

Because the resistivity of ZnO NWs ($\approx 5\ \Omega$ cm)[14] is much higher than that of Au ($2.4 \times 10^{-6}\ \Omega$ cm), the electrical field, and then the cathode overpotential on the NW surface, is lower than that on the Au electrodes. Therefore, the reduction of copper ions is more difficult on the NW than on the electrodes. Figure 4 indicates the embedding process of the ZnO NW during electrodeposition in different plating baths. When using copper nitrate solution, copper

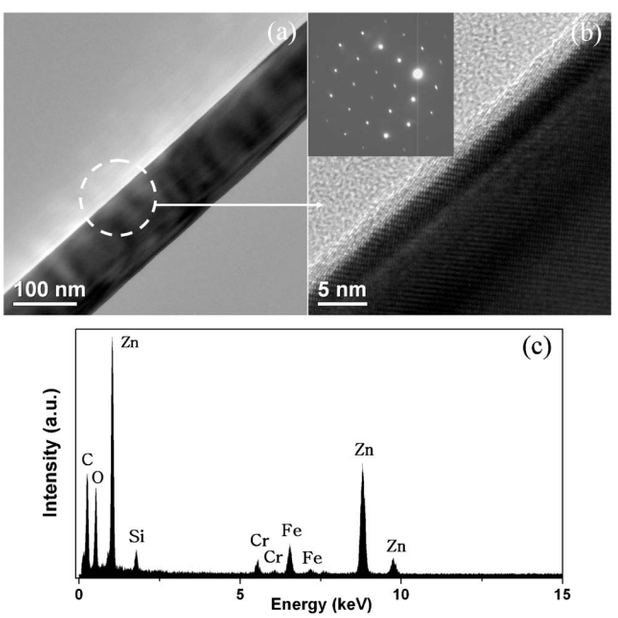

Figure 3. (a) TEM image of a ZnO NW after electrodeposition using copper nitrate solution. The ZnO NW was transferred onto a molybdenum grid for TEM observation from the wafer after electrodeposition. (b) High-resolution TEM image and corresponding electron diffraction pattern recorded from the edge of the NW. (c) One of the EDS spectra recorded from the ZnO NW. The results of (a)–(c) indicate that the ZnO NW surface is clean of copper.

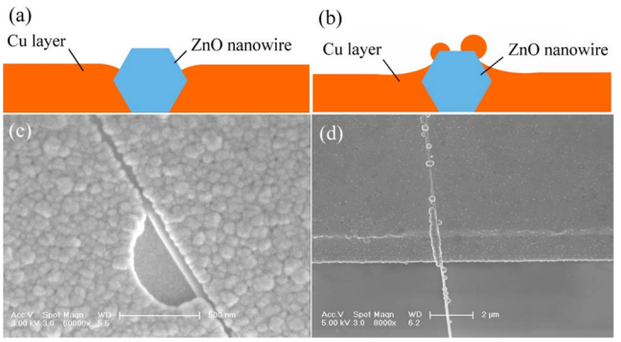

Figure 4. (Color online) (a) and (b) Schematics of the embedding process of ZnO NW using copper nitrate bath and pyrophosphate bath. (c) SEM image of embedded ZnO NW on the electrode using copper nitrate bath, showing that the NW was embedded in copper coating gradually. Region A was insulated by celluloid to prevent copper deposition for observation. (d) SEM image of embedded ZnO NW using pyrophosphate bath, showing that copper was deposited on the electrodes and NW surface simultaneously.

deposition can only occur on the Au electrode surface due to the low covering power of the solution. With the growth of the coating, the ZnO NW was gradually embedded in copper at the contact sides, as shown in Fig. 4a and c. However, with much higher covering power than the copper nitrate bath,[15] the pyrophosphate bath can neglect the difference of the cathode overpotential between the NW and the Au electrodes. Therefore, copper deposits on both the metal electrodes and the NW surface simultaneously in the pyrophosphate bath, as shown in Fig. 4b and d.

The overall electrical resistance of the devices can be significantly reduced by the selective electrodeposition process, as shown in Fig. 5, which presents the measurements on the same device

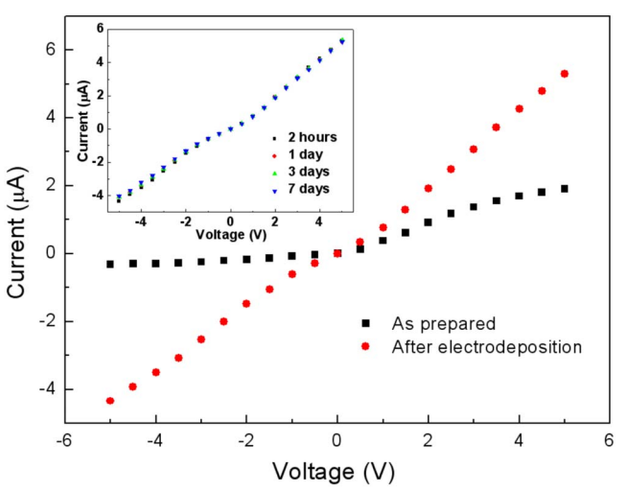

Figure 5. (Color online) *I-V* characteristics of the ZnO NW device before and after electrodeposition using copper nitrate solution, showing the contact improvement of the device by selective electrodeposition. After electrodeposition, the device was rinsed with deionized water, followed by drying at 60°C for 1 h. The inset is the *I-V* characteristics of a ZnO NW device at different times after electrodeposition using copper nitrate solution, showing the stability of the device. Measurements were done at room temperature.

before and after selective electrodeposition using copper nitrate solution. Without the treatment, the as-fabricated device exhibits a rectifying current-voltage (*I-V*) characteristic. However, the device showed a linear *I-V* curve after electrodeposition, and the current flowing through the NW was increased greatly, 3–10 times. The inset in Fig. 5 shows the measurements of the same device at different time intervals after selective electrodeposition. The measurement performed 7 days later is consistent with the data obtained 2 h after the sample was made, indicating the stability of the device made by selective electrodeposition.

In summary, single ZnO NW devices were fabricated by a selective copper electrodeposition process. The electroadsorption phenomenon of ZnO NWs was investigated and served as a pretreatment process of electrodeposition to avoid the desorption of the NW as it immerged in the electrolyte. The covering power of the electroplating bath was found to have a significant effect on the metal deposition process. A pyrophosphate bath with high covering power results in copper depositing on both the electrodes and the NW surface. A copper nitrate bath with low covering power can be used to achieve selective metal deposition only at the electrode surface, rather than the surface of the NW, which will be eventually embedded at the contact region only with the growth of copper coating. This provides an effective method for fabricating NW/NB/nanotube-based devices in general, such as carbon nanotubes. We believe that, by combining with dielectrophoresis and other self-assembly techniques, this method has the potential to be useful in large-scale production of one-dimensional nanomaterial-based devices.

Acknowledgments

The authors are thankful to Professor Wen H. Ko at Case Western Reserve University for his helpful discussions. This work was supported by China Postdoctoral Science Foundation (20070420382).

Tsinghua University assisted in meeting the publication costs of this article.

References

1. K. Keem, D. Y. Jeong, S. Kim, M. S. Lee, I.-S. Yeo, U.-I. Chung, and J.-T. Moon, *Nano Lett.*, **6**, 1454 (2006).
2. C. S. Lao, J. Liu, P. X. Gao, L. Y. Zhang, D. Davidovic, R. Tummala, and Z. L. Wang, *Nano Lett.*, **6**, 263 (2006).
3. C. Soci, A. Zhang, B. Xiang, S. A. Dayeh, D. P. R. Aplin, J. Park, X. Y. Bao, Y. H. Lo, and D. Wang, *Nano Lett.*, **7**, 1003 (2007).
4. Z. Fan and J. G. Lu, *Appl. Phys. Lett.*, **86**, 123510 (2005).
5. Q. Wan, Q. H. Li, Y. J. Chen, T. H. Wang, X. L. He, J. P. Li, and C. L. Lin, *Appl. Phys. Lett.*, **84**, 3654 (2004).
6. C. S. Lao, M. C. Park, Q. Kuang, Y. L. Deng, A. K. Sood, D. L. Polla, and Z. L. Wang, *J. Am. Chem. Soc.*, **129**, 12096 (2007).
7. Y. W. Heo, B. S. Kang, L. C. Tien, D. P. Norton, F. Ren, J. R. L. A. Roche, and S. J. Pearton, *Appl. Phys. A: Mater. Sci. Process.*, **80**, 497 (2005).
8. D. Wang, C. J. Otten, W. E. Buhro, and J. G. Lu, *IEEE Trans. Nanotechnol.*, **3**, 328 (2004).
9. T. Brintlinger, M. S. Fuhrer, J. Melngailis, I. Utke, T. Bret, A. Perentes, P. Hoffmann, M. Abourida, and P. Doppelt, *J. Vac. Sci. Technol. B*, **23**, 3174 (2005).
10. J. Kjelstrup-Hansen, S. Dohn, D. N. Madsen, K. Molhave, and P. Boggild, *J. Nanosci. Nanotechnol.*, **6**, 1995 (2006).
11. S. Dohn, J. Kjelstrup-Hansen, D. N. Madsen, K. Molhave, and P. Boggild, *Ultramicroscopy*, **105**, 209 (2005).
12. Z. W. Pan, Z. R. Dai, and Z. L. Wang, *Science*, **291**, 1947 (2001).
13. C. M. A. Brett and A. M. O. Brett, *Electrochemistry: Principles, Methods and Applications*, p. 113, Oxford University Press, New York (1993).
14. Y. W. Heo, L. C. Tien, D. P. Norton, B. S. Kang, F. Ren, B. P. Gila, and S. J. Pearton, *Appl. Phys. Lett.*, **85**, 2002 (2004).
15. F. A. Lowenheim, *Modern Electroplating*, p. 199, John Wiley & Sons, New York (1974).